IP has become the switching technology of our twenty-first-century broadband networks, including both the Internet and mobile communication networks since 4G. We will, however, resist the urge to delve any further into IP so that we do not stray too far into networking, which, although extremely exciting, is beyond the scope of this book.

13.4 Code Division Multiplexing

CDM is based on *spread spectrum modulation*, a technique that was developed in the 1940s for military communications. The message signal, of (unspread) bandwidth B_m, is spread in a pseudorandom manner over a bandwidth $B_c >> B_m$. The bandwidth ratio

$$G = \frac{B_c}{B_m} \tag{13.17}$$

represents a processing gain, which accounts for an increase in the signal-to-noise ratio at the output of a spread spectrum receiver. Transmitting a signal by spread spectrum modulation yields important benefits.

- The signal is immune to intentional interference, called *jamming*. A high-power jamming signal is necessarily narrowband and will fail to drown the information signal since only a small fraction of the signal energy is corrupted. More accurately, the process of spread spectrum demodulation at the receiver involves the use of a pseudorandom code, which de-spreads the wanted signal back into a narrow band B_m. Interestingly, the effect of this process on the jamming signal is to spread it over a wide band B_c. In this way, the jamming signal energy is rendered insignificant within the narrow band occupied by the recovered wanted signal.
- By a similar consideration, spread spectrum signals are immune to frequency-selective fading arising from multipath propagation.
- An unauthorised receiver cannot recover the information signal from the transmitted spread spectrum signal. Simply put, you must have knowledge of the carrier frequency in order to tune into a transmission. And if, as in an equivalent view of spread spectrum, the carrier frequency is not fixed but changes pseudorandomly then the oscillator frequency at the receiver must change exactly in step for demodulation to be possible. Only authorised receivers will know precisely the pseudorandom sequence of carrier frequencies used at the transmitter.
- Spread spectrum signals have a noise-like appearance to other (unauthorised) receivers. Thus, multiple user transmissions can simultaneously occupy the same frequency band with guaranteed message privacy, provided each user's signal has been spread using a unique pseudorandom code, also referred to as *pseudonoise* (PN) sequence. This is CDM, which is finding increased nonmilitary applications in satellite and mobile cellular communications. Clearly, as the number of users increases a point is reached where the 'background noise' at each receiver becomes excessive leading to unacceptable bit error ratios (BERs).

13.4.1 Types of Spread Spectrum Modulation

There are various types of spread spectrum (SS) modulation depending on the method employed to spread the message signal over a wider bandwidth.

- *Time-hopping* (TH): the message signal is transmitted in bursts during pseudorandomly selected time slots. Figure 13.34a shows the block diagram of a TH transmitter. Let R_m denote the bit rate of the encoded message signal, giving a bit interval $T_m = 1/R_m$, and a message bandwidth $B_m = R_m$. Each time interval $T >> T_m$ is divided into L equal time slots, and one of these slots is selected pseudorandomly (by opening the gate for this duration) for transmission. To keep up with the message rate, we must take from the buffer an average of R_m

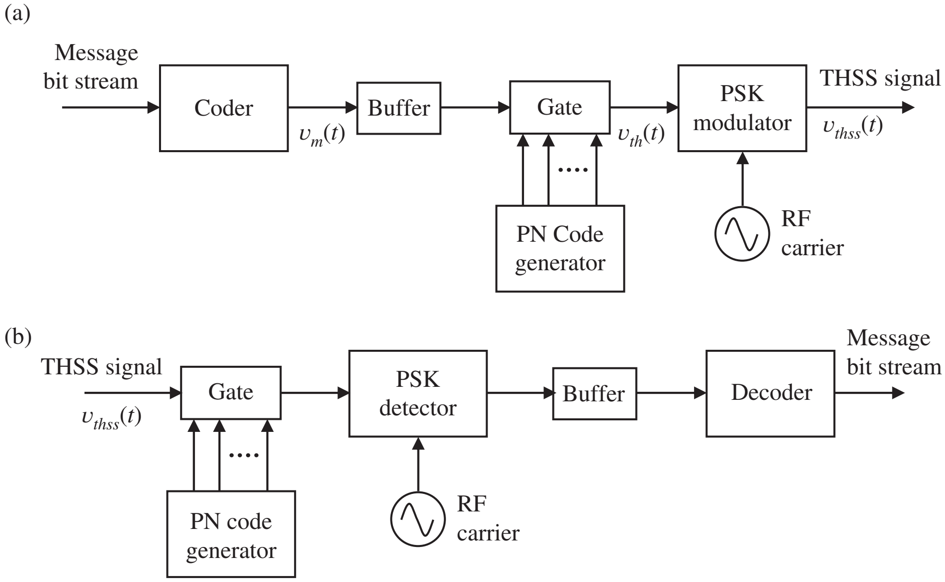

Figure 13.34 Time-hopping spread spectrum (THSS): (a) transmitter; (b) receiver.

bits per second, or $R_m T$ bits in each interval T, which must all be sent during the one time slot (of duration T/L) when the gate is open. Thus, the burst bit rate is

$$R_s = \frac{R_m T}{T/L} = LR_m$$

With PSK modulation, the transmission bandwidth is $B_c = LR_m$, which gives processing gain $G = L$.
A TH receiver is shown in Figure 13.34b. The gate must be opened in precise synchronism with the transmitter, which requires that (i) the gate is controlled by the same PN code used at the transmitter and (ii) both codes are in phase. This synchronisation is very stringent and becomes more difficult to achieve as L increases. Note that the role of the buffer at the receiver is to play out the demodulated bursty bit stream at the uniform rate of the coded message signal.

- *Frequency-hopping* (FH): the message signal is conveyed on a carrier, which hops pseudorandomly from one frequency to another, making R_h hops per second. Figure 13.35a shows a block diagram of a frequency-hopping spread spectrum (FHSS) transmitter. A coded message bit stream first FSK modulates a carrier signal, which is then multiplied in a mixer by a digital frequency synthesiser output, and the sum frequency is selected. The output frequency f_o of the synthesiser is controlled by a PN sequence taken k bits at a time. Noting that an all-zero combination does not occur in a PN sequence, we see that there are $L = 2^k - 1$ different values over which f_o hops. The FSK modulator generates symbols at a rate R_s – one symbol per bit for binary FSK, or per $\log_2 M$ bits for M-ary FSK. If the hop rate R_h is an integer multiple of the symbol rate R_s, several frequency hops occur during each symbol interval. This type of FHSS is known as *fast-frequency hopping*. If, however, $R_h \le R_s$, then one or more symbols are transmitted on each hop, and we have *slow-frequency hopping*.
  At the receiver (Figure 13.35b), exactly the same pseudorandom sequence of frequencies f_o is generated and used in a mixer to remove the frequency hopping imposed on the FSK signal. It is extremely difficult for frequency synthesisers to maintain phase coherence between hops, which means that a noncoherent FSK demodulator must be used at the receiver. The main advantages of FHSS are that synchronisation requirements are less stringent, and larger spread spectrum bandwidths can be more easily achieved to realise higher processing gains $G \approx 2^k - 1$.

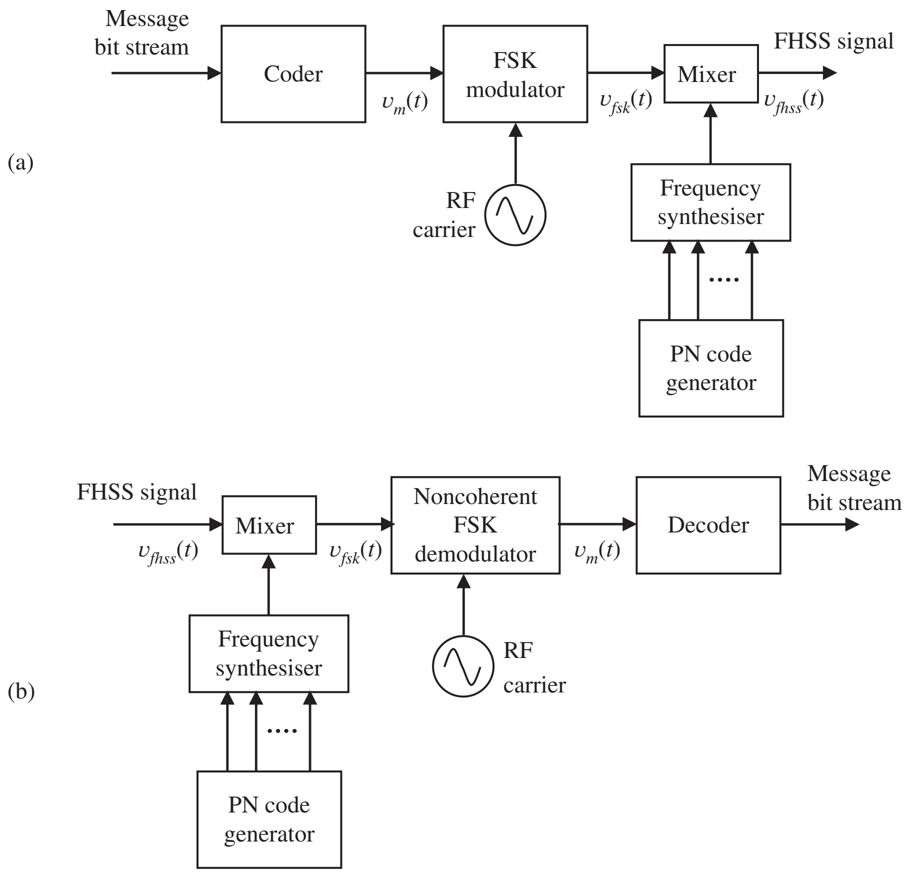

Figure 13.35 Frequency-hopping spread spectrum (FHSS): (a) transmitter; (b) receiver.

- *Direct sequence* (DS): the coded message signal, of bit duration T_m, is multiplied by a PN bit stream of much shorter bit duration T_c, referred to as *chip duration*. This pseudorandomises the message bit stream and spreads its (null) bandwidth from $B_m = 1/T_m$ to $1/T_c$, which yields a processing gain

$$G = T_m/T_c \tag{13.18}$$

  This highly spread product signal is then used to modulate a carrier by BPSK, QPSK, or M-ary APSK. *Direct sequence spread spectrum* (DSSS) is the type of spread spectrum modulation employed in CDM-based mobile cellular communication (e.g. the old standard IS-95), and our discussion of CDM will be restricted to this method. One disadvantage of DSSS (compared to FHSS) is that the processing gain that can be achieved is limited by current device technology as T_m decreases (in high information rate systems), since the required low values of T_c become difficult to implement. Timing requirements in DSSS are also more stringent than in FHSS, but less than in *time-hopping spread spectrum* (THSS).
- *Hybrid methods*: hybrid SS techniques are possible that combine TH, FH, and DS. The most common hybrid technique is DS/FH, which combines the large processing gain possible in FH with the advantage of coherent detection in DS. Each frequency hop carries a DS spread spectrum signal and is coherently detected, but the signals from different hops have to be incoherently combined because of their lack of phase coherence.

13.4.2 CDM Transmitter

Figure 13.36a shows the block diagram of a CDM transmitter based on DSSS modulation. The waveforms associated with this transmitter are shown in Figure 13.36b. Unit-amplitude bipolar waveforms are assumed for convenience. The coded message waveform $v_m(t)$ has the indicated bit duration T_m, whereas the PN waveform $v_{pn}(t)$ has a chip duration T_c. Note that the waveforms correspond to the case $T_m = 15T_c$. More than one user (say N) can be accommodated, with each assigned a unique PN code $v_{pn1}(t)$, $v_{pn2}(t)$, …, $v_{pnN}(t)$, or a unique time shift in a common PN code $v_{pn}(t - \tau_1)$, $v_{pn}(t - \tau_2)$, …, $v_{pn}(t - \tau_N)$.

The PN code generator is in general a linear feedback shift register. Figure 13.37a shows the circuit connection that produces the PN sequence $v_{pn}(t)$ used in Figure 13.36b. The shift register consists of four flip-flops (FF1 to FF4), which are controlled by a common clock. Clock pulses occur at intervals of T_c, and at each clock pulse the input state of each flip-flop is shifted to its output. The outputs of FF1 and FF4 are added in an EX-OR gate and fed back as input to the shift register. This gate performs a modulo-2 addition defined as follows

$$\begin{aligned} 0 &\oplus 0 = 0 \\ 0 &\oplus 1 = 1 \\ 1 &\oplus 0 = 1 \\ 1 &\oplus 1 = 0 \end{aligned} \tag{13.19}$$

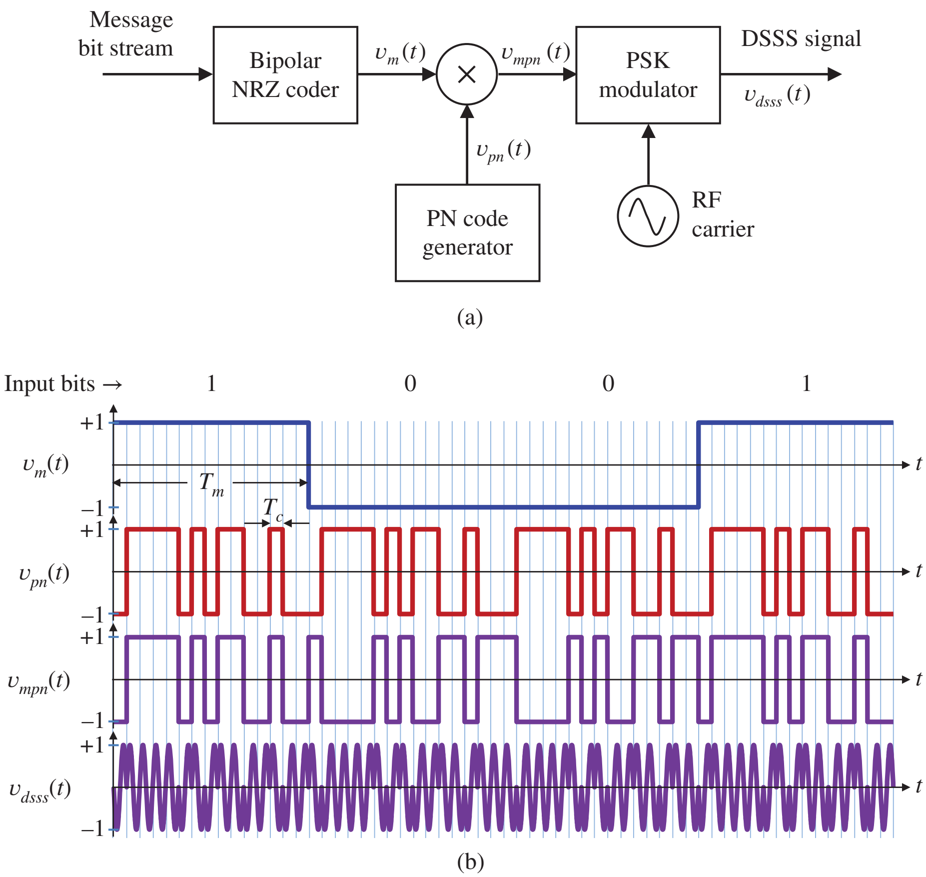

Figure 13.36 Direct sequence spread spectrum: (a) transmitter; (b) waveforms.

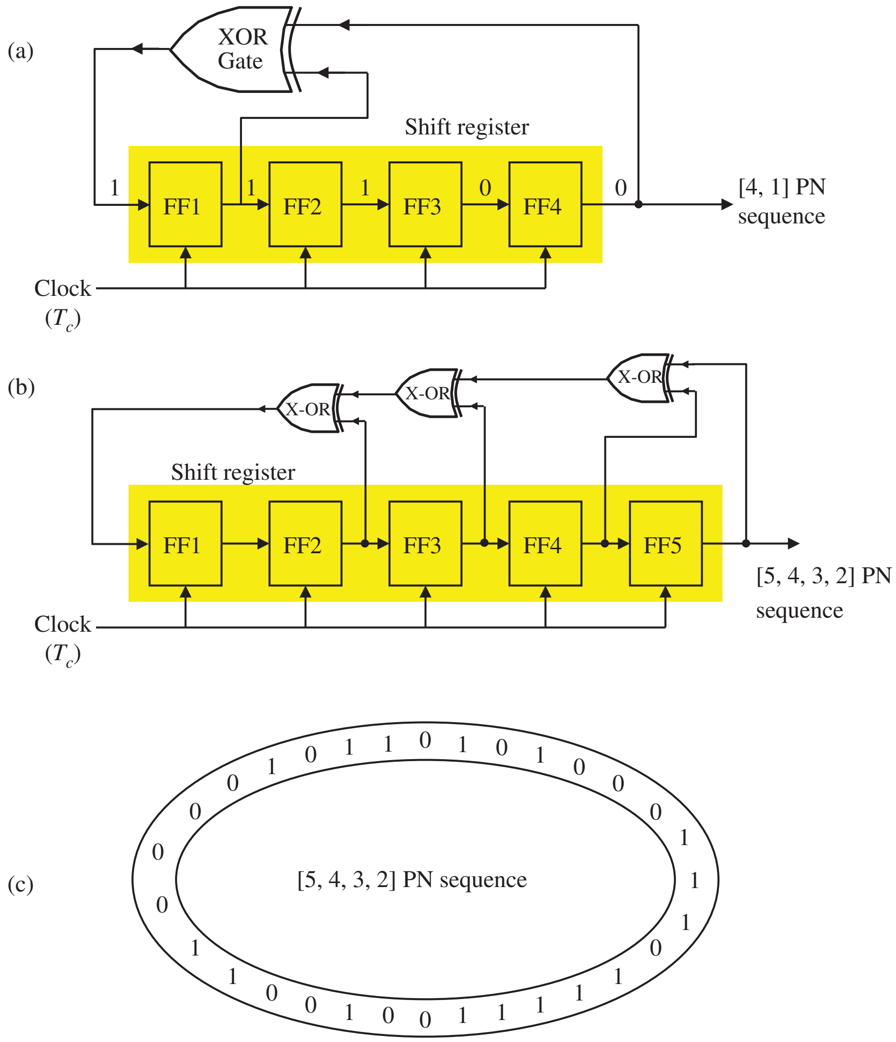

Figure 13.37 Maximum-length PN sequence: (a) generator of the [4, 1] code listed in Table 13.2; (b) [5, 4, 3, 2] code generator; (c) [5, 4, 3, 2] code.

Because the feedback taps are located at the outputs of the fourth and first flip-flops, we have what is known as a [4, 1] code generator. In general, a linear feedback shift register that consists of m flip-flops and has feedback taps at the outputs of flip-flops $m, i, j, \ldots$ is identified as $[m, i, j, \ldots]$. The serial PN code generated is of course the sequence of states of the m^{th} flip-flop. As an example, Figure 13.37b shows the connection of a [5, 4, 3, 2] PN code generator, which gives the cyclic pseudorandom sequence shown in (c). The following discussion clarifies how this sequence is obtained.

Let us assume that the [4, 1] PN code generator in Figure 13.37a has the indicated *initial* register state (FF1, FF2, FF3, FF4) = (1, 1, 0, 0). This is the state before the first clock pulse occurs at time $t = 0$. The initial feedback input is therefore FF1 $\oplus$ FF4 = 1.

Table 13.2 lists the sequence of flip-flop outputs. After the first clock pulse at $t = 0$, the initial feedback state is shifted to become the FF1 output, the initial FF1 output becomes FF2 output, etc. Thus, the register state just after

Table 13.2 Sequence of flip-flop outputs in [4, 1] PN code generator.

Time (t)	Input to shift register (Feedback)	Flip-flop Output			
		FF1	FF2	FF3	FF4 (PN sequence)
<0	1	1	1	0	0
0	1	1	1	1	0
T_c	0	1	1	1	1
$2T_c$	1	0	1	1	1
$3T_c$	0	1	0	1	1
$4T_c$	1	0	1	0	1
$5T_c$	1	1	0	1	0
$6T_c$	0	1	1	0	1
$7T_c$	0	0	1	1	0
$8T_c$	1	0	0	1	1
$9T_c$	0	1	0	0	1
$10T_c$	0	0	1	0	0
$11T_c$	0	0	0	1	0
$12T_c$	1	0	0	0	1
$13T_c$	1	1	0	0	0
$14T_c$	1	1	1	0	0
$15T_c$	1	1	1	1	0

$t = 0$ is (1, 1, 1, 0), and the feedback state is $1 \oplus 0 = 1$. This gives the entry 1, 1, 1, 1, 0 in row $t = 0$ of the table. You may wish to carry on in this way and verify the remaining entries of Table 13.2, and then skip to Question 13.3 for more practice. Note in Table 13.2 that the register goes through all possible 2^4 states, except the all-zero state (0, 0, 0, 0), before starting all over again at $t = 15T_c$. In general, a PN sequence (generated by a linear feedback register of m flip-flops) that has the maximum period

$$L = (2^m - 1) \quad \text{Clock cycles} \tag{13.20}$$

is called a *maximum-length sequence*, or simply an *m-sequence*. The all-zero state is forbidden and in fact cannot be entered except from an all-zero initial state, which would then cause the register to remain permanently in this state, and the PN sequence to be a train of 0's. Note further that the periodic code sequence generated by a linear feedback shift register is fixed entirely by the number of flip-flops m and the feedback tap locations. The initial state of the register merely determines the starting point of the cycle.

13.4.3 CDM Receiver

A CDM receiver is shown in Figure 13.38a. There are two stages of processing. First, the spread signal $v_{mpn}(t)$ is extracted by coherent PSK detection. The PSK detector consists of a product modulator followed by a lowpass filter of bandwidth equal to that of $v_{mpn}(t)$. Further details of PSK detection are given in Chapter 11 but are not required for this discussion. The second stage of processing involves a correlation receiver (discussed in Chapter 12). This multiplies $v_{mpn}(t)$ by a locally generated code, which must be identical to and exactly in step with the

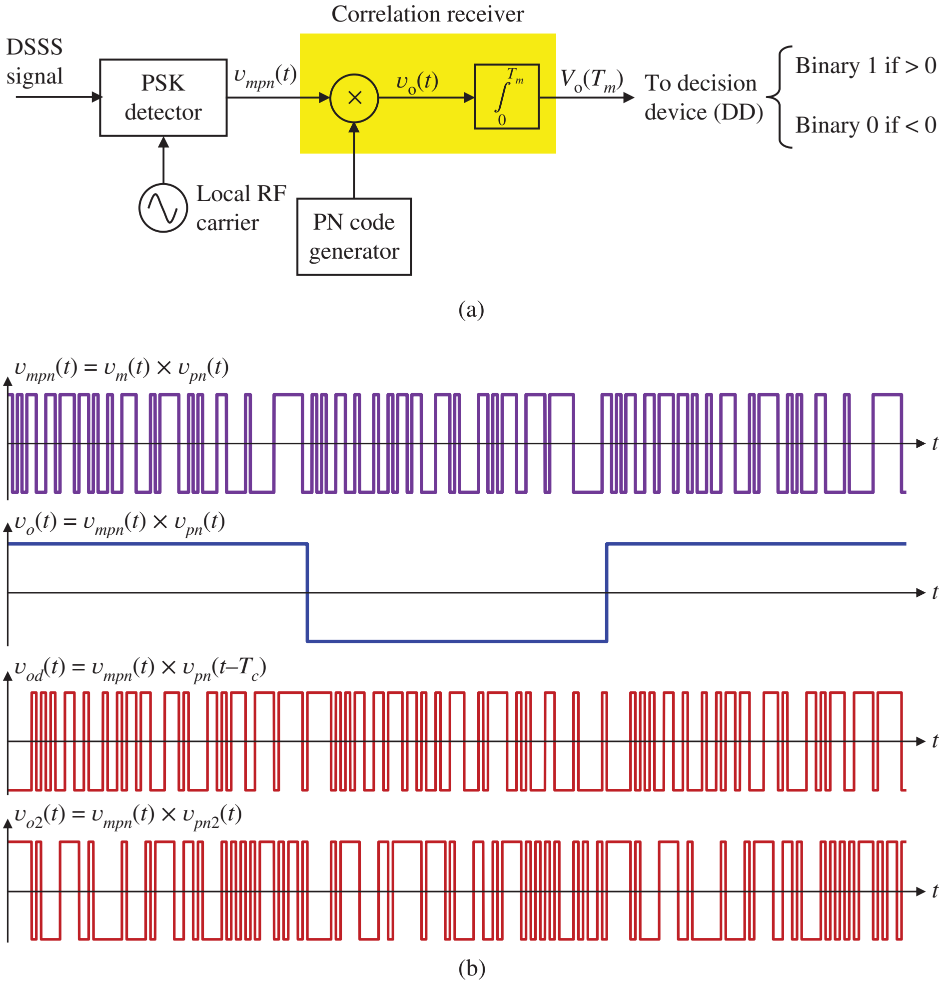

Figure 13.38 Direct sequence spread spectrum: (a) receiver; (b) waveforms of indicated signals. (Note: $v_{mpn}(t)$ corresponds to message signal segment $v_m(t)$ = 101 spread using $v_{pn}(t)$ = Code [6, 1]; and $v_o(t)$, $v_{od}(t)$, and $v_{o2}(t)$ are the results of de-spreading using locally generated codes, where $v_{pn2}(t)$ = Code [6, 5, 2, 1].)

code $v_{pn}(t)$ used at the transmitter. The multiplication yields a de-spread signal $v_o(t)$, which is then integrated in regular intervals of one message bit duration T_m. A decision device compares the integration result $V_o(T_m)$ in each interval to a zero threshold. The (message) bit interval is declared to contain a binary 1 if $V_o(T_m)$ exceeds zero. A decision in favour of binary 0 is taken if $V_o(T_m)$ is less than zero, and a random guess of 1 or 0 is made if $V_o(T_m)$ is exactly equal to zero.

An illustration of the operation of the receiver is given in Figure 13.38b. The waveform $v_{mpn}(t)$ corresponds to a message bit stream segment $v_m(t) \equiv 101$ that was spread at the transmitter using $v_{pn}(t)$ = Code [6, 1]. Multiplying $v_{mpn}(t)$ with a perfectly synchronised Code [6, 1] yields $v_o(t)$. Clearly, this process has somehow extracted the original waveform $v_m(t)$ from a signal $v_{mpn}(t)$ that is noise-like in appearance. You can see that this is the case by noting that $v_{pn}(t) = \pm 1$, so that

$$v_{pn}^2(t) = 1 \tag{13.21}$$

Hence

$$\begin{aligned} v_o(t) &= v_{mpn}(t)v_{pn}(t) \\ &= [v_m(t)v_{pn}(t)]v_{pn}(t) \\ &= v_m(t)[v_{pn}^2(t)] \\ &= v_m(t) \end{aligned} \tag{13.22}$$

The importance of synchronisation is illustrated in the waveform $v_{od}(t)$, which is the result of using the right code [6, 1] but with a misalignment of one chip duration T_c. In addition, we illustrate in $v_{o2}(t)$ the effect of using a wrong code $v_{pn2}(t) =$ Code [6, 5, 2, 1]. Proceeding as in Eq. (13.22), we write

$$\begin{aligned} v_{od}(t) &= v_m(t)[v_{pn}(t)v_{pn}(t - T_c)] \\ v_{o2}(t) &= v_m(t)[v_{pn}(t)v_{pn2}(t)] \end{aligned} \tag{13.23}$$

You can see that in these two cases we have failed to de-spread $v_{mpn}(t)$ since the term in brackets is not a constant but just another PN code (i.e. a random sequence of ± 1). The input to the integrator is therefore a randomised version of the original signal $v_m(t)$, the spreading signal being the term in brackets. It means that $v_m(t)$ remains hidden, and the integrator sees only noise-like signals $v_{od}(t)$ and $v_{o2}(t)$. By examining these two waveforms you can see that the decision device will make random guesses of 1 or 0, since the average of these waveforms in intervals of T_m is approximately zero. Note that the process of integration is equivalent to averaging except for a scaling factor.

Figure 13.39 illustrates the code misalignment problem more clearly. Here the output $V_o(T_m)$ of the correlation receiver is plotted against misalignment τ. With perfect synchronisation between transmitter and receiver codes, $\tau = 0$ and $V_o(T_m) = E_m$ for binary 1 and $-E_m$ for binary 0, where E_m is the energy per message bit. We see that the noise margin (i.e. difference between the output levels of the correlation receiver for binary 1 and 0 in the absence of noise) is $2E_m$. As τ increases, the noise margin decreases steadily causing increased BER, and reaching zero – with $V_o(T_m) = 0$ and BER = 0.5 – at

$$\tau = \frac{L}{L+1}T_c \tag{13.24}$$

Here $L = 2^m - 1$ is the length of the PN code and m is the length of the linear feedback register that generates the code. For a misalignment of T_c or larger we have

$$V_o(T_m) = \begin{cases} -E_m/L, & \text{Binary 1} \\ +E_m/L, & \text{Binary 0} \end{cases} \tag{13.25}$$

That is, the noise margin is $-2E_m/L$, which is negative and implies that in a noiseless receiver a binary 1 would always be mistaken for binary 0, and vice versa. However, a practical receiver will always be subject to noise and, because L is large, the value $V_o(T_m) = \pm E_m/L$ will be negligible compared to noise. Thus, the input to the decision device will simply fluctuate randomly about 0 according to the variations of noise. Under this scenario, the output of the decision device will be a random sequence of bits 1 and 0 so that BER = 50%, which is what you get in the long run from random guesses in a binary sample space. It is important to note that these comments are only applicable to a misalignment in the range $T_c \le \tau \le (L-1)T_c$. Beyond $(L-1)T_c$, the two codes will begin to approach perfect alignment at $\tau = LT_c$ due to their cyclic sequence.

We have demonstrated above that a message signal can only be recovered from a spread spectrum signal in a receiver equipped with a synchronised correct PN code. We now demonstrate with the aid of Figure 13.40 that a receiver will also correctly extract its desired signal from a multitude of spread spectrum signals. We show two message waveforms $v_{m1}(t) \equiv 101$ and $v_{m2}(t) \equiv 001$, which have been spread using different PN codes $v_{pn1}(t)$ and

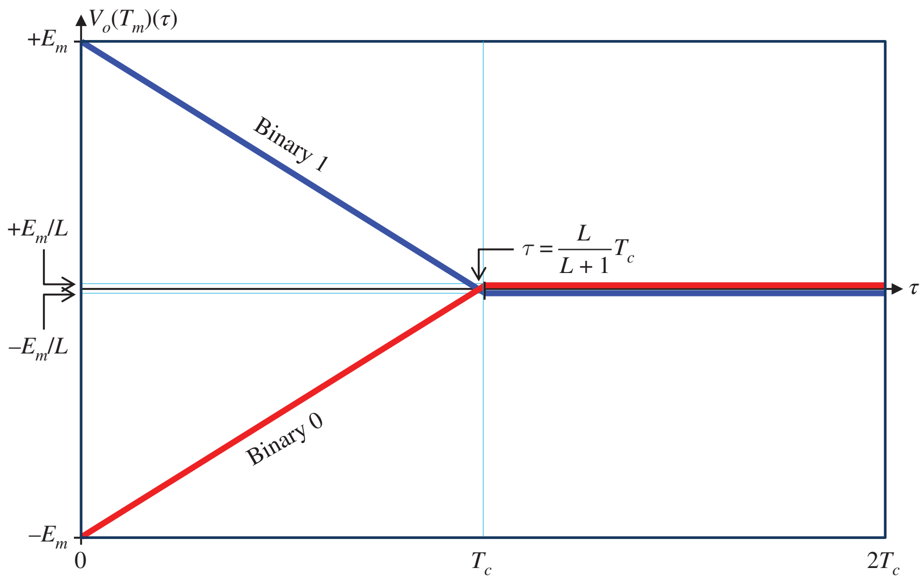

Figure 13.39 Output $V_o(T_m)$ of correlation receiver as a function of PN code misalignment τ.

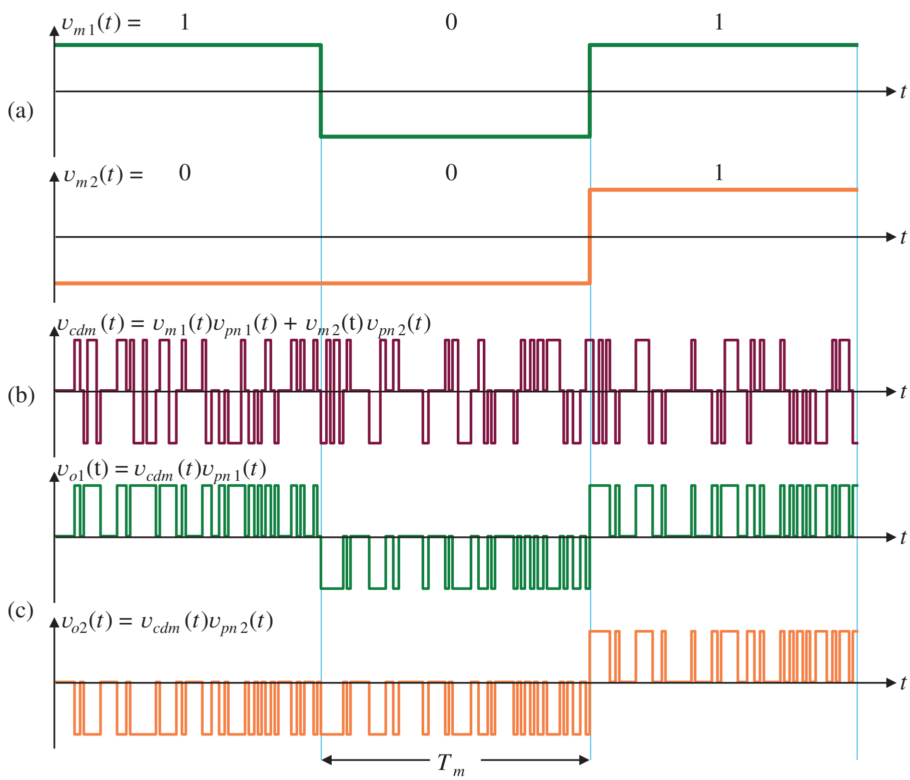

Figure 13.40 Two-channel CDM example showing (a) user data waveforms $v_{m1}(t)$ and $v_{m2}(t)$, (b) received CDM waveform $v_{cdm}(t)$, and (c) waveforms $v_{o1}(t)$ and $v_{o2}(t)$ after each channel at the receiver multiplies $v_{cdm}(t)$ by its allotted PN code.

$v_{pn2}(t)$ assigned to users 1 and 2, respectively. Thus, the signal at the receiver of each user (at the output of the PSK detector) is a composite signal given by

$$v_{cdm}(t) = v_{m1}(t)v_{pn1}(t) + v_{m2}(t)v_{pn2}(t) \tag{13.26}$$

Receiver 1 multiplies $v_{cdm}(t)$ by its unique code $v_{pn1}(t)$, whereas receiver 2 multiplies by $v_{pn2}(t)$ to obtain

$$\begin{aligned} v_{01}(t) &= v_{m1}(t) + v_{m2}(t)v_{pn2}(t)v_{pn1}(t) \\ v_{02}(t) &= v_{m2}(t) + v_{m1}(t)v_{pn1}(t)v_{pn2}(t) \end{aligned} \tag{13.27}$$

These waveforms are also plotted in Figure 13.40 from which we see that integrating each one over every message bit interval will lead to correct decisions regarding the transmitted bit streams. That is, each receiver successfully extracts only the bit stream intended for it from the mix of bit streams contained in the CDM signal $v_{cdm}(t)$. This is a remarkable result. In general, the signal at the input of a receiver in a CDM system with N simultaneous transmissions is given by

$$v_{cdm}(t) = v_{m1}(t)v_{pn1}(t) + v_{m2}(t)v_{pn2}(t) \ + \cdots + \ v_{mN}(t)v_{pnN}(t) \tag{13.28}$$

The de-spread signal of, say, receiver 1 is therefore

$$\begin{aligned} v_{o1}(t) &= v_{cdm}(t)v_{pn1}(t) \\ &= v_{m1}(t) + v_{m2}(t)v_{pn2}(t)v_{pn1}(t) \ + \cdots + \ v_{mN}(t)v_{pnN}(t)v_{pn1}(t) \\ &= v_{m1}(t) + \text{Noise} \end{aligned} \tag{13.29}$$

Similar results apply to every one of the N receivers. The situation is therefore reduced to the familiar problem of digital signal detection in noise. As the number of users N goes up, the noise term in Eq. (13.29) becomes larger, and the probability of error, or BER, increases. So, there is a limit on the number of users in order to guarantee a specified BER. To quantify this limitation, consider an N-user CDM system in which the same signal power P_s reaches the receiver from each user. The unwanted accompanying $N-1$ CDM signals constitute noise in addition to the receiver noise power P_n, but typically $P_s >> P_n$. The carrier-to-noise ratio $(C/N)_i$ of the wanted signal at the receiver input is thus

$$(C/N)_i = 10\log_{10}\left(\frac{P_s}{P_n + (N-1)P_s}\right) \quad \simeq \quad 10\log_{10}\left(\frac{1}{(N-1)}\right) \quad \text{dB}$$

De-spreading by the receiver adds a processing gain G given earlier in Eq. (13.17), so that the carrier-to-noise ratio C/N of the de-spread signal (which is the signal from which a demodulator will attempt to recover the original bit stream) increases to

$$\begin{aligned} C/N &= (C/N)_i + 10\log_{10}(G) \\ &= 10\log_{10}\left(\frac{G}{(N-1)}\right) \quad \simeq \quad 10\log_{10}\left(\frac{G}{N}\right) \quad \text{dB} \end{aligned} \tag{13.30}$$

We see therefore that G must be much larger than the number of users N if this C/N is to meet the threshold needed by the demodulator to achieve a specified BER. We may rearrange the above equation to obtain number of users N in terms of G and C/N

$$N = \frac{G}{10^{(C/N)/10}} \tag{13.31}$$

For example, assuming that the transmission system includes error control coding which allows the BER at demodulator output to be as high as 10^{-2} (because it is followed by a codec that reduces BER from this high value to an acceptable 10^{-7}) then we can determine minimum C/N needed by a QPSK modem as follows. We read from Figure 11.45 the value of E_b/N_o needed to achieve BER 10^{-2}. This gives $E_b/N_o = 4.32$. We then convert this value to C/N, assuming an ideal modem (with no implementation loss) and an ideal Nyquist filter (i.e. a raised cosine filter with roll-off factor $\alpha = 0$) and recalling that QPSK is M-ary PSK with $M = 4$. Thus

$$\begin{aligned} C/N &= 4.32 + 10\log_{10}(\log_2 M) = 4.32 + 10\log_{10}(2) \\ &= 7.33\ \text{dB} \end{aligned}$$

So, in this case, Eq. (13.31) gives $N = G/5.41$. This means that to accommodate 100 users we would need $G = 541$, which means that we require a 541-fold increase in bandwidth (from message bandwidth to the bandwidth of the transmitted CDM signal), and this could be a significant barrier. Alternatively, this means that chip duration T_c must be $(1/541)^{\text{th}}$ the message bit duration T_m and this may be difficult to achieve with available technology if message bit rate is high.

13.4.4 Crucial Features of CDM

Let us conclude our discussion of CDM by emphasising those features that are crucial to the smooth operation of this multiplexing strategy.

13.4.4.1 Synchronisation

The PN code generated at the receiver must be identical to and synchronised with the spreading code used at the transmitter. There is usually no problem with the two codes being identical – unless of course the receiver is unauthorised – so we concentrate on the synchronisation requirement. Let the transmitter code be $v_{pn}(t)$ and the receiver code $v_{pn}(t - \tau)$ – with a misalignment τ. It follows from the receiver block diagram that

$$\begin{aligned} V_o(T_m) &= \int_0^{T_m} v_{mpn}(t) v_{pn}(t-\tau) dt \\ &= \int_0^{T_m} v_m(t) v_{pn}(t) v_{pn}(t-\tau) dt \\ &= \pm \frac{E_m}{T_m} \int_0^{T_m} v_{pn}(t) v_{pn}(t-\tau) dt \\ &= \pm E_m R_p(\tau) \end{aligned} \tag{13.32}$$

In the above we have used the fact that $v_m(t)$ is a (normalised) constant $\pm E_m/T_m$ in the integration interval spanning one message bit interval. The positive sign applies to binary 1 and the negative sign to binary 0. $R_p(\tau)$ is the *autocorrelation* function of a periodic signal – in this case $v_{pn}(t)$ – of period T_m and is defined by

$$R_p(\tau) = \frac{1}{T_m} \int_0^{T_m} v_{pn}(t) v_{pn}(t-\tau) dt \tag{13.33}$$

The autocorrelation function of a signal has several interesting properties, which we discuss in Section 3.5.5. Equation (13.33) has been evaluated for a normalised unit-amplitude maximum-length PN sequence of length L and chip duration T_c, and is shown in Figure 13.41. By examining this figure, we see the importance of synchronisation. Equation (13.32) states that the output of the correlation receiver is proportional to $R_p(\tau)$, which from Figure 13.41 is clearly maximum at $\tau = 0$ and decreases rapidly to $-1/L$ at $\tau = T_c$. You may wish to look back at Figure 13.39 and note that it is actually a plot of Eq. (13.32).

In practice, synchronisation is accomplished at the receiver in two stages. First is the *acquisition* stage, also known as *coarse synchronisation*, which is performed at the start of signal reception, or after loss of synchronisation, by sliding the timing of the locally generated PN code until a peak output is obtained. To do this the PN code first modulates a carrier, as was done in the transmitter. The resulting signal is then correlated with the incoming spread spectrum signal, and the code alignment is shifted until maximum correlation is achieved. Next follows the *tracking* stage or *fine synchronisation* in which a phase-locked loop is used to keep the locally generated PN code in step with the transmitter code.

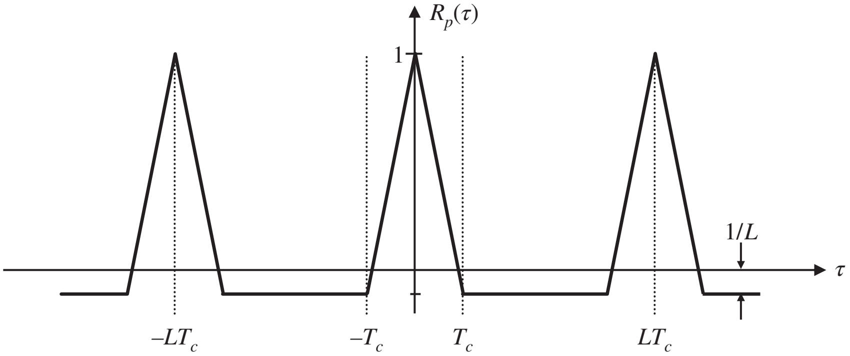

Figure 13.41 Autocorrelation of a maximum-length PN sequence of length L and chip duration T_c.

13.4.4.2 Cross-correlation of PN Codes

Returning to Eq. (13.29), which deals with the detection of a spread spectrum signal in a multi-user environment, we see that the correlation output of receiver 1 may be written as

$$\begin{aligned}V_{o1}(T_m) &= \int_0^{T_m} v_{cdm}(t)v_{pn1}(t)dt\\ &= \int_0^{T_m} [v_{m1}(t)v_{pn1}(t) + v_{m2}(t)v_{pn2}(t-\tau_2) \;\; + \cdots + \;\; v_{mN}(t)v_{pnN}(t-\tau_N)]v_{pn1}(t)dt\\ &= \pm E_{m1} \pm \frac{E_{m2}}{T_m}\int_0^{T_m} v_{pn1}(t)v_{pn2}(t-\tau_2)dt \pm \cdots \pm \frac{E_{mN}}{T_m}\int_0^{T_m} v_{pn1}(t)v_{pnN}(t-\tau_N)dt\\ &= \pm E_{m1} \pm E_{m2}R_{12}(\tau_2) \pm \cdots \pm E_{mN}R_{1N}(\tau_N)\end{aligned} \tag{13.34}$$

Here, τ_k (for $k = 2, 3, \ldots, N$) is the misalignment between receiver 1 and the PN code of the k^{th} user transmission. And $R_{1k}(\tau)$ is the cross-correlation function of the PN sequences $v_{pn1}(t)$ and $v_{pnk}(t)$, defined by

$$R_{1k}(\tau) = \frac{1}{T_m}\int_0^{T_m} v_{pn1}(t)v_{pnk}(t-\tau)dt \tag{13.35}$$

Equation (13.34) shows that for there to be no interference between users in a CDM system, the cross-correlation of any two PN codes in the system must be zero. Equivalently, we say that the PN sequences should be mutually *orthogonal*. This requirement is impossible to meet in practice, and we can only search for classes of PN codes that give acceptably small (i.e. good) cross-correlation. Figure 13.42 shows the cross-correlation of maximum-length PN sequences [5, 2] versus [5, 4, 3, 2], and [7, 1] versus [7, 6, 5, 4, 2, 1]. A class of codes known as *Gold sequences* gives better cross-correlation properties. A Gold sequence results from an EX-OR combination of two carefully selected m-sequences. In general (and this is apparent from Figure 13.42), the larger the sequence length L, the smaller the cross-correlation, which leads to reduced mutual interference. However, processing delay (for example during coarse synchronisation) increases with L.

13.4.4.3 Power Control

By examining Eq. (13.34) we see that our failure to find a class of PN codes with zero cross-correlation leads to stringent power control requirements in order to minimise mutual interference in a multi-user CDM system. To be more specific, consider a receiver such as a base station in CDM-based cellular telephony or a satellite transponder that employs a CDM-based multiple access. This receiver is equipped with N correlators, one for each of the N user transmissions. Let $V_{oj}(T_m)$ denote the output of correlator j and E_{mj} the energy per message bit reaching the receiver from the j^{th} user. It is clear that the unwanted contribution to $V_{o1}(T_m)$ from the other user

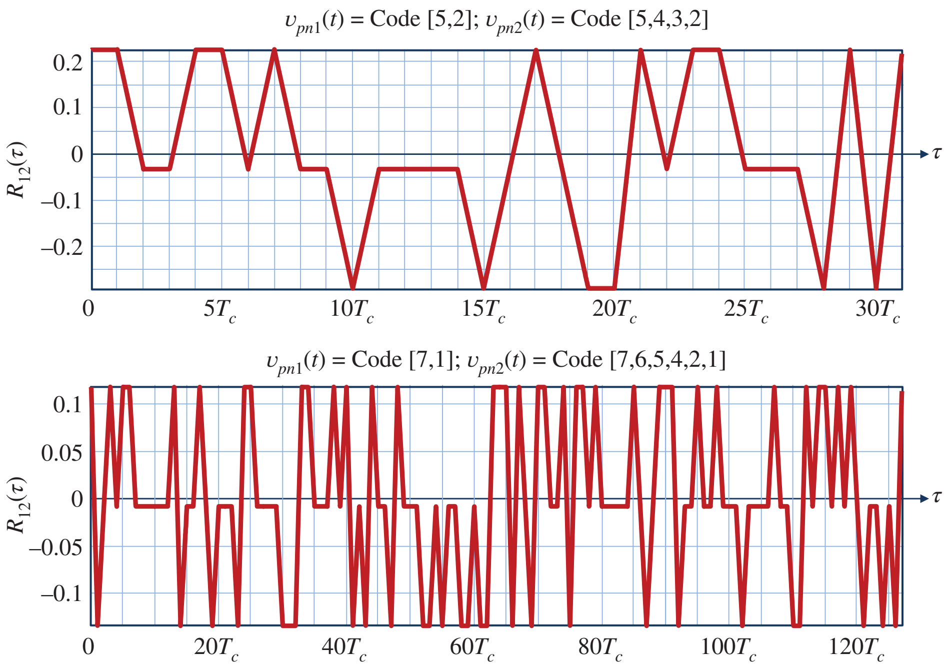

Figure 13.42 Cross-correlation $R_{12}(\tau)$ of maximum-length PN sequences.

transmissions will depend on $E_{m2}, E_{m3}, \ldots, E_{mN}$ according to Eq. (13.34). Similarly, the unwanted contribution to $V_{o2}(Tm)$ depends on $E_{m1}, E_{m3}, \ldots, E_{mN}$. And so on. You can therefore see that the condition for minimum mutual interference is that

$$E_{m1} = E_{m2} = E_{m3} = \cdots = E_{mN} \tag{13.36}$$

That is, the transmission from each of the N users must reach the receiver at the same power level. As the radio link from each user to the receiver is typically of a different length and subject to different propagation conditions, we must implement some form of power control in order to achieve Eq. (13.36).

One way of implementing power control is by each user terminal monitoring the level of a *pilot signal* from the base station and adjusting its transmitted power level accordingly. A low pilot level indicates high path loss between terminal and base station, perhaps because the two are far apart, and causes the terminal to increase its transmitted power level. A high pilot level, on the other hand, indicates low path loss, perhaps due to increased proximity between user terminal and base station and causes the terminal to reduce its transmitted power. This technique is known as *open loop power control*. It assumes identical propagation conditions in the two directions of transmission between terminal and base station, which will often not be the case for a mobile terminal or if the pilot signal is at a different frequency from the user transmission. For example, if the monitored pilot signal undergoes a frequency-selective fade, the user terminal could overestimate the path loss experienced by its transmissions to the base station, which would cause it to increase its transmitted power excessively. There could also be situations when the user terminal grossly underestimates the attenuation on its transmissions to the base station because it is in a deep fade, whereas the pilot signal is not.

Closed loop power control solves the above problem but requires a higher operational overhead. Here, the base station monitors the transmission from each terminal and regularly issues a command that causes the terminal to increase or decrease its transmitted power. For example, a one-bit command could be issued every 1.25 ms. A binary 1 indicates that the power transmitted by the terminal is too high, the terminal responding by decreasing its power by 1 dB. A binary 0 indicates that the power reaching the base station from the terminal is too low, and in response the terminal increases its radiated power by 1 dB. The power transmitted by a base station is also controlled based on *power measurement reports* received from user terminals, which indicate the signal strength reaching each terminal and the number of detected bit errors.

13.4.4.4 Processing Gain

It is illuminating to examine PN codes in the frequency domain in order to make important observations on their signal processing roles. The autocorrelation function $R_p(\tau)$ of an m-sequence $v_{pn}(t)$ was sketched in Figure 13.41. The Fourier transform of $R_p(\tau)$ gives the power spectral density $S_p(f)$ of $v_{pn}(t)$, which furnishes complete information on the frequency content of the PN sequence. We obtain $S_p(f)$ readily from the waveform of $R_p(\tau)$ by noting that $R_p(\tau)$ is a centred triangular pulse train of period $T = LT_c$, pulse width $2T_c$, and hence duty cycle $d = 2T_c/LT_c = 2/L$. The pulse train has amplitude $A = 1 + 1/L$ and has been reduced (shifted vertically down) by a constant level $1/L$. From Chapter 4 (see, for example, Eq. (4.19)), we know that this waveform has the following Fourier series

$$R_p(\tau) = \frac{Ad}{2} - \frac{1}{L} + Ad\sum_{n=1}^{\infty} \text{sinc}^2(nd/2)\cos(2\pi n f_o \tau); \quad f_o = \frac{1}{T}$$

Substituting the above values, we obtain

$$R_p(\tau) = \frac{1}{L^2} + \frac{2(L+1)}{L^2}\sum_{n=1}^{\infty} \text{sinc}^2(n/L)\cos(2\pi n f_o \tau); \quad f_o = \frac{1}{LT_c}$$

This indicates that $R_p(\tau)$ has DC component of amplitude $A_o = 1/L^2$ and contains harmonics spaced apart by frequency $f_o = 1/LT_c$, with the n^{th} harmonic (of frequency nf_o) having amplitude A_n given by

$$A_n = \frac{2(L+1)}{L^2}\text{sinc}^2(n/L)$$

This, being the spectrum of the autocorrelation function $R_p(\tau)$ of the PN sequence, is the PSD of the sequence and is shown in Figure 13.43 for $L = 15$. This spectrum provides valuable information.

A PN sequence $v_{pn}(t)$ contains sinusoidal components of frequencies up to a (null) bandwidth equal to the reciprocal of the chip duration T_c. You may recall from Chapter 7 that the effect of multiplying a baseband signal by a sinusoid of (carrier) frequency f_c is to shift the baseband spectrum to be centred at f_c. Furthermore, the frequency translation may be removed without distortion to the baseband spectrum simply by performing the multiplication a second time using a carrier of the same frequency and phase. Thus, multiplying a message bit stream $v_m(t)$ by a PN sequence will duplicate (in other words spread) the spectrum of $v_m(t)$ at intervals of $1/LT_c$ over a bandwidth of $1/T_c$. A little thought will show that the duplicated spectra are diminished in amplitude in proportion to T_c, and that they overlap each other. The composite spread spectrum is therefore roughly uniform (somewhat like that of white noise) and bears little resemblance to the baseband spectrum, which means that the signal has been successfully hidden. Overlapping of the duplicated spectra is important; otherwise, the situation reduces to the straightforward process of sampling where the spectra are distinguishable and the 'spreading' can be removed by lowpass filtering. We ensure overlapping by using a spreading sequence that has a dense spectrum – implying a small value of $1/LT_c$. For a given chip duration T_c, this requires that we make the sequence length L very large.

A second multiplication by $v_{pn}(t)$ at the receiver has the 'magical' effect of reconstructing the message signal spectrum, because the spectra originally translated to $f = k/LT_c$, $k = 1, 2, 3, \ldots, L$ are simply thrown back to $f = 0$, and these all add to give the original baseband spectrum. This is provided the 'carrier frequencies' k/LT_c have the same phases at transmitter and receiver, which is another way of saying that the two PN codes must be synchronised. You will recall that a time shift of τ on $v_{pn}(t)$ has the effect of altering the phases of its frequency components by $2\pi f\tau$. Yes, the multiplication also creates new spectra at $2\,k/LT_c$, but these are filtered out.

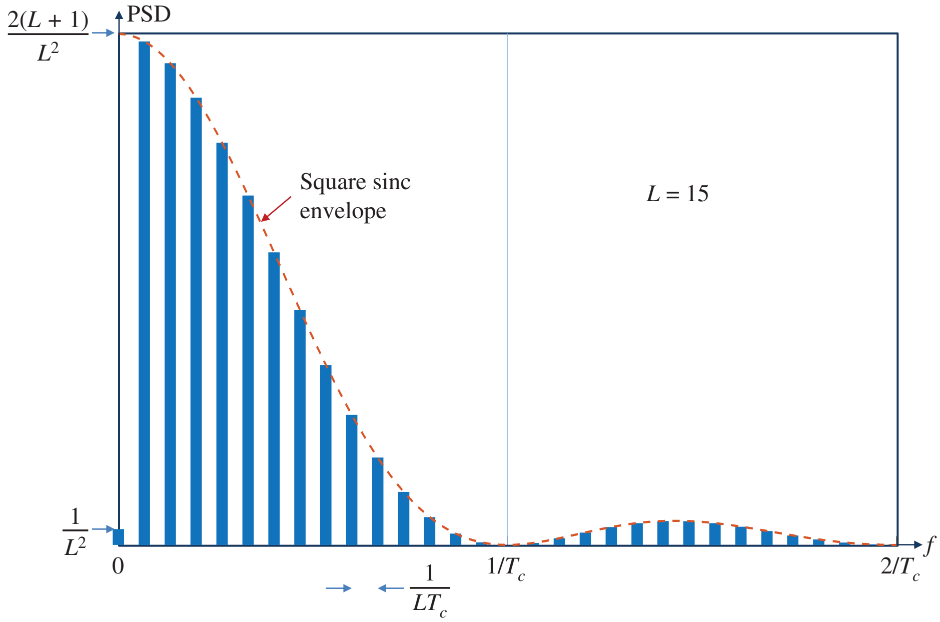

Figure 13.43 PSD of PN sequence of length $L = 15$.

Herein lies the spread spectrum processing gain. For interference signals entering the receiver along with the wanted signal, this is their first multiplication with this code, which therefore spreads them over a bandwidth $1/T_c$. However, for the wanted signal it is the second multiplication, and this returns its frequency components back to the (null) bandwidth $1/T_m$, where T_m is the message bit interval. Clearly then, the C/N at the output of the de-spreader is larger than the C/N at the input by the amount

$$\begin{aligned}\text{Processing Gain} &= 10\log_{10}\left(\frac{T_m}{T_c}\right), \quad \text{dB} \\ &= 10\log_{10}\left[\frac{\text{Spread (null) bandwidth (Hz)}}{\text{Message bit rate (b/s)}}\right], \quad \text{dB}\end{aligned} \tag{13.37}$$

For example, if a spread bandwidth of 1.23 MHz is employed to transmit at a message bit rate of 9.6 kb/s, Eq. (13.37) gives a processing gain of 21.1 dB. For a given message bit rate, processing gain can be increased to realise improved performance in the presence of noise and interference by using a larger spread bandwidth $1/T_c$. But allocated radio bandwidths are limited, and device technology places a limit on how small we can make the chip duration T_c.

13.5 Multiple Access

Each of the main multiplexing strategies discussed in this chapter may be utilised as a multiple access technique. It is important to note the distinction between multiplexing and multiple access. Multiplexing is the process of combining multiple user signals for simultaneous transmission as a composite signal on one transmission link, whereas multiple access is concerned with how one communication resource such as a satellite transponder or a terrestrial base station is shared by various transmitting stations, each operating on a separate transmission link. Although the concept is more generally applicable, we will limit our brief discussion to a satellite communication application of multiple access. There are three main types of multiple access, namely frequency division multiple access (FDMA), time division multiple access (TDMA), and code division multiple access (CDMA).

13.5.1 FDMA

In FDMA, each transmitting earth station (ES) is allocated a separate frequency band in the satellite transponder. Figure 13.44 illustrates the sharing of a 36 MHz transponder among three earth stations (ESs). Each ES is allocated an exclusive 10 MHz bandwidth, which is used for simultaneous and continuous transmission as required. Note that a composite FDM signal exists on the downlink, whereas the uplink has separate links, each operating on a separate carrier frequency. To allow the use of realisable filters when extracting a desired channel from the downlink FDM signal, FDMA always includes a guard band (GB) between allocated adjacent sub-bands. In the illustration, a GB of 2 MHz is used. The signal transmitted by each ES may contain a single user signal or it may be a multiplex of several user signals. The former is known as *single channel per carrier* (SCPC) and the latter as *multiple channel per carrier* (MCPC).

FDMA is very simple and cheap to implement using well-established filter technology, but it is prone to intermodulation distortion when the transponder amplifier is operated in its nonlinear region. To reduce this distortion, a lineariser is often used to pre-distort the incoming signal at the transponder in such a way as to make up for the subsequent amplification distortion. Additionally, input power is reduced from the level that would saturate the amplifier – an action known as *back-off* – by the amount (in dB) necessary to ensure operation in a linear region of the transfer characteristic of the combined lineariser/amplifier system.

FDMA capacity may be readily determined in terms of the number of ESs N that can share a transponder bandwidth B_{xp} with each station needing bandwidth B_{es} and a GB B_g maintained between allocated sub-bands

$$N = \left\lfloor \frac{B_{xp}}{B_{es} + B_g} \right\rfloor \tag{13.38}$$

The bandwidth requirement B_{es} of each transmission depends on the required bit rate and the modulation scheme employed. These relationships are summarised in Section 11.11. Power issues must be considered when

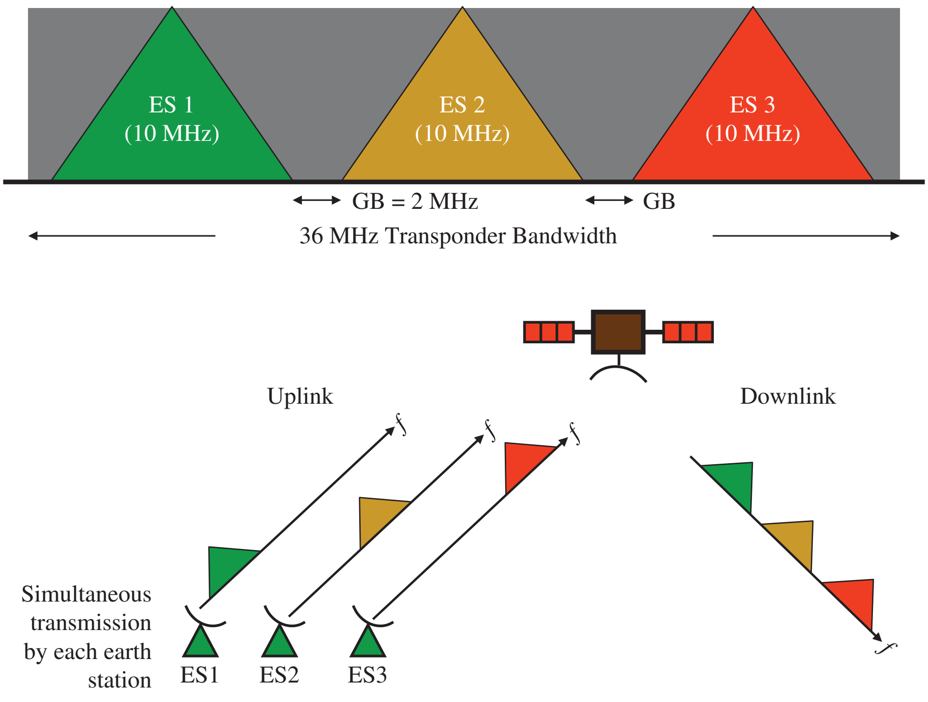

Figure 13.44 FDMA concept.

assessing capacity because, while there may be enough bandwidth to accommodate N stations, there may be insufficient power to support that number at the required C/N. When considering power in FDMA, it must always be remembered that a receiving ES shares the advertised transponder power (i.e. satellite transmit effective isotropically radiated power (EIRP)) only in proportion to the ES's allocated bandwidth (as a fraction of transponder bandwidth).

13.5.2 TDMA

The concept of TDMA is illustrated in Figure 13.45. ESs take turns in making use of the entire transponder bandwidth by transmitting bursts of RF signals within centrally allocated and nonoverlapping time slots. If N transmitting ESs share the transponder then over an interval known as a *frame duration* T_f, each station is allocated one time slot for its burst transmission. Therefore, on the uplink, there are separate transmission links operating at the same frequency but at different time intervals, and on the downlink there is the TDMA frame carrying the signal of each of the N stations in separate time slots. A frame duration may range from 125 μs up to 20 ms, but a value of 2 ms is common. A large frame duration yields high frame efficiency but increases delay and complexity. It is always necessary to include a guard time between each time slot to ensure that bursts from stations using adjacent time slots will not overlap in their arrival time at the satellite even if there is a slight variation in the arrival of each burst. Such small variations in arrival time may be caused by timing error at the ES, changes in the distance between an ES and the satellite, and changes in propagation condition.

TDMA is not affected by intermodulation distortion since only one carrier is present in the transponder at any given time. This is an advantage because it allows amplifiers to be operated at their maximum capacity, which saves on bulk and weight (since one no longer must use a larger amplifier at a reduced output due to back-off). However, each ES must transmit at a high symbol rate (to fill the transponder bandwidth) and must do so using

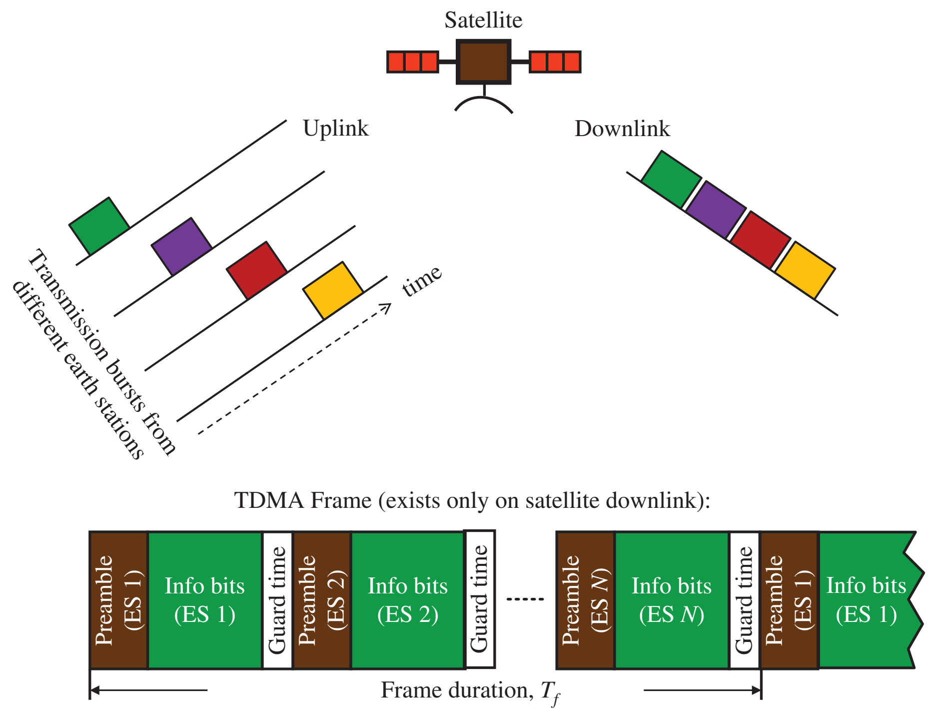

Figure 13.45 TDMA concept.

enough signal power to provide an acceptable C/N, taking into consideration the proportionate increase in noise power with bandwidth as N_oB. For this reason, TDMA is not as suitable as FDMA for transmitting narrowband signals from small ESs.

TDMA capacity, in terms of the number of stations N that can share a transponder of bandwidth B_{xp} using a TDMA frame of duration T_f and guard time T_g between time slots and number of preamble bits n_{bp} in each station's transmit burst, may be determined in several ways. One way is to start by specifying the required bit rate R_{es} of each station, the M-ary modulation scheme (APSK or PSK) and the raised cosine filter roll-off factor α. This sets the burst bit rate as

$$R_{burst} = \frac{B_{xp}}{(1+\alpha)}\log_2 M \tag{13.39}$$

The duration of the time slot T_{es} needed by each ES within the TDMA frame of duration T_f is

$$T_{es} = \frac{R_{es}T_f}{R_{burst}} \tag{13.40}$$

We must also allow a total guard time NT_g within the frame as well as total time NT_p for all stations to send their preamble bits, where

$$T_p = \frac{n_{pb}}{R_{burst}} \tag{13.41}$$

Since $NT_{es} + NT_g + NT_p = T_f$, it follows that the TDMA system capacity is

$$N = \left\lfloor \frac{T_f}{T_g + T_{es} + T_p} \right\rfloor \tag{13.42}$$

where T_f and T_g are in the system specification, and T_{es} and T_p are calculated using the preceding equations.

Worked Example 13.2

A TDMA system has the following specifications:

- Satellite transponder bandwidth, $B_{xp} = 72$ MHz.
- TDMA frame duration, $T_f = 2$ ms.
- Guard time between time slots, $T_g = 1$ μs.
- Number of preamble bits in each ES burst, $n_{bp} = 148$ bits.

Determine the number of stations that can be accommodated if each station operates at a bit rate $R_{es} = 20$ Mb/s (which includes redundancy due to error control coding) using 16-APSK and a raised cosine filter of roll-off $\alpha = 0.05$.

Determine also the TDMA frame efficiency.

The supported burst bit rate is

$$R_{burst} = \frac{B_{xp}}{(1+\alpha)}\log_2 M = \frac{72}{1.05} \times 4 = 274.286 \text{ Mb/s}$$

Required time slot per station per frame is

$$T_{es} = \frac{R_{es}T_f}{R_{burst}} = \frac{20 \times 2}{274.286} = 0.1458 \text{ ms}$$

Required time for preamble per station per frame is

$$T_p = \frac{n_{pb}}{R_{burst}} = \frac{148}{274.286} = 0.5396 \ \mu\text{s}$$

The number of stations is therefore

$$N = \left\lfloor \frac{T_f}{T_g + T_{es} + T_p} \right\rfloor = \left\lfloor \frac{2}{1 \times 10^{-3} + 0.1458 + 0.5396 \times 10^{-3}} \right\rfloor$$
$$= \lfloor 13.57 \rfloor$$
$$= 13$$

Frame efficiency is the fraction of the frame duration that is devoted to carrying bits from the N stations. Since, in this case, in every 2 ms we have 13 stations using 0.1458 ms each to transmit their data, frame efficiency is

$$\eta = \frac{NT_{es}}{T_f} \times 100\% = \frac{13 \times 0.1458}{2} \times 100\%$$
$$= 94.79\%$$

This TDMA efficiency is quite high. In practical systems, the guard time will be higher than 1 μs and the number of preamble bits will be larger. This will reduce frame efficiency and hence system capacity.

13.5.3 CDMA

In CDMA, each transmitting ES multiplies its signal by a unique orthogonal spreading code prior to transmission. These signals reach the satellite transponder at the same time and in the same frequency band. Following frequency down conversion and power amplification, a composite CDM signal is transmitted on the satellite downlink, containing N differently spread signals from the sharing ESs. The theoretical details of the CDM signal generation and detection are as discussed under CDM. Figure 13.46 shows a CDMA system consisting of N transmit ESs. Details of the receiver operations on the incoming downlink signal from the satellite in order to recover

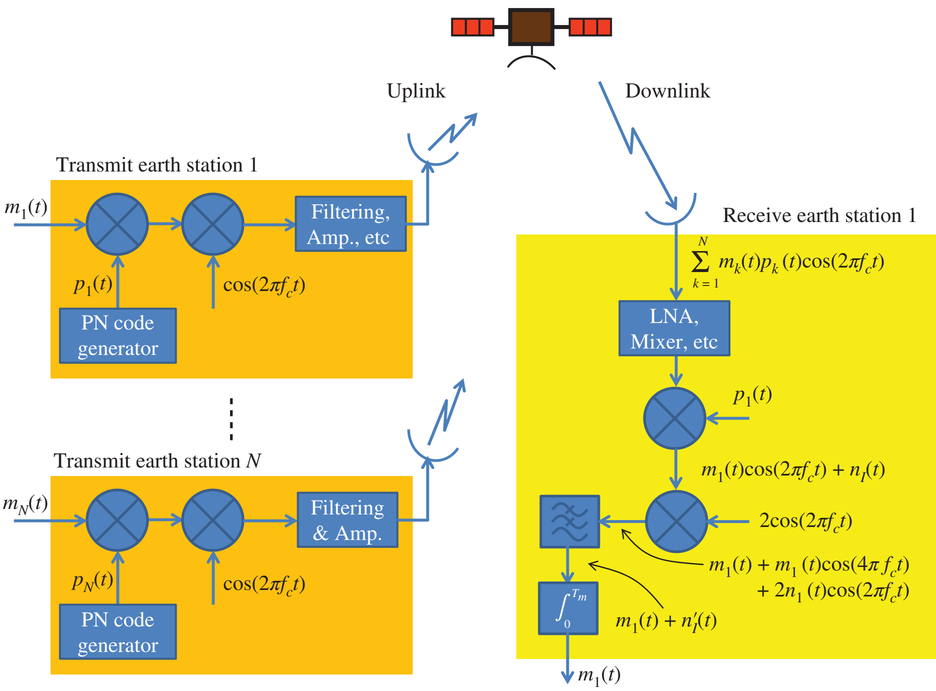

Figure 13.46 CDMA system operation.

the wanted message signal from any of the N stations are also given in the diagram, using Earth Station 1 as an example.

CDMA has several benefits, such as helping to reduce interference from co-channel systems, since the unwanted carrier signals will be spread and therefore mostly rejected by the receiver. It also serves to reduce multipath effect since the reflected waves will be spread by the receiver if their delay exceeds a chip duration. Also, unlike TDMA, coordination between ESs sharing one transponder is not required, although synchronisation of the spreading sequences at transmitter and receiver is essential, as discussed in Section 13.4. Theoretically, CDMA facilitates 100% frequency reuse between beams in a multiple spot beam satellite system. However, CDMA's main drawback is its low efficiency, expressed in terms of the total achievable data rate of a CDMA system utilising an entire transponder when compared to the data rate of a single carrier that fully occupies the same transponder. We did earlier discuss the constraint on CDMA capacity and derived Eq. (13.31) for number of users in terms of processing gain and C/N. CDMA requires a large contiguous bandwidth in order to achieve the high processing gain required, and this may not be available on a satellite transponder. Furthermore, strict power control must be maintained, as also earlier discussed.

13.5.4 Hybrid Schemes

The multiple access techniques discussed above are often used in combination. For example, a satellite transponder bandwidth may be divided into sub-bands and each sub-band is shared by multiple small ESs using TDMA. This combination of FDMA and TDMA is known as *multifrequency TDMA* (MF-TDMA). An example is shown in Figure 13.47, where 12 stations share one transponder which has been partitioned into three sub-bands denoted f_1, f_2, and f_3. Four stations share each sub-band using a TDMA frame with four allocated time slots. Note therefore that the system resource allocated in FDMA is a frequency band, and in TDMA it is a time slot, but in MF-TDMA

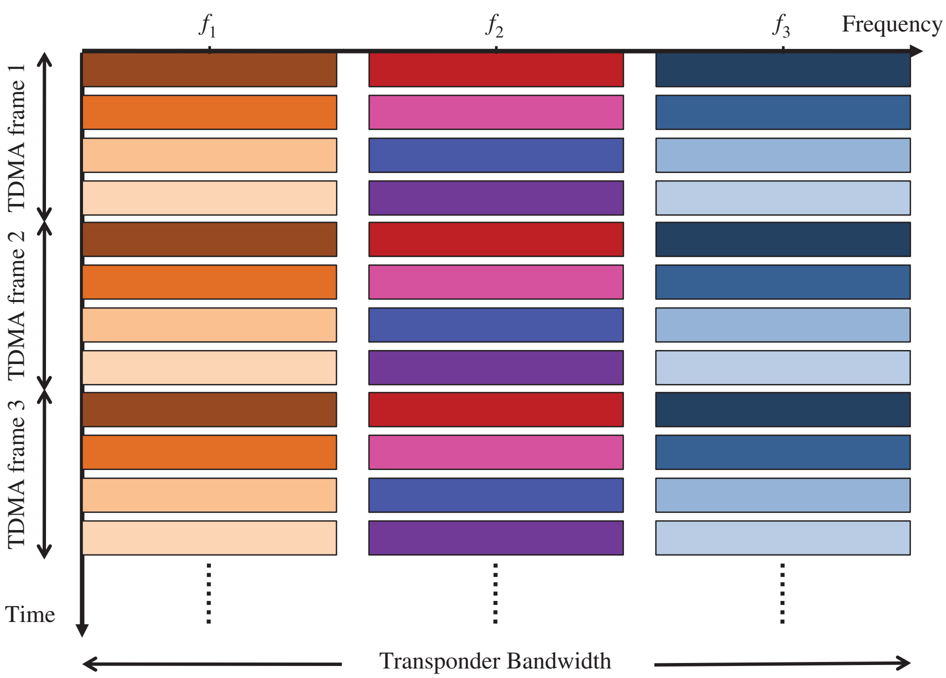

Figure 13.47 Example of 12 stations sharing one transponder using MF-TDMA.

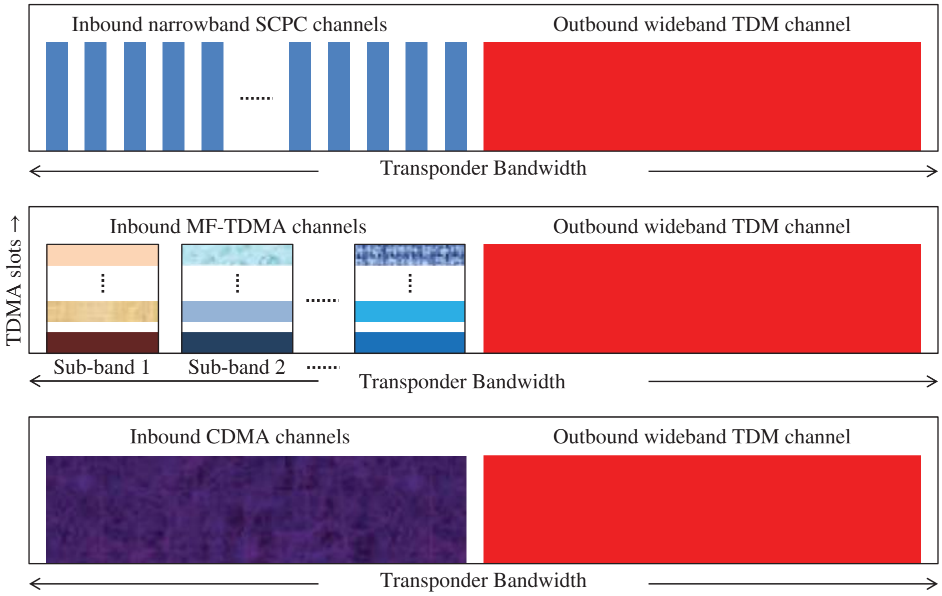

Figure 13.48 Hybrid multiple access schemes for a star VSAT network.

the allocation is both a time slot and a frequency band. This allocation is usually dynamic and according to need and may change in a time interval of a few frames.

Figure 13.48 shows three hybrid multiple access arrangements for a VSAT (very small aperture terminal) star network implementation. In all three scenarios, half of the transponder bandwidth is used to carry a wideband TDM signal on the outbound link (from the hub station to the VSAT terminals) and the other half is used for the inbound link supporting transmissions from multiple VSAT terminals to the hub. These VSATs share their half of the transponder bandwidth using three different schemes: SCPC FDMA is used in the top scenario, MF-TDMA is used in the middle, and CDMA is used in the bottom. Note therefore that the bottom scenario is a combination of CDMA and FDMA, the top scenario is pure FDMA but with unequal sub-band partitioning, whereas the middle scenario is a combination of MF-TDMA and FDMA.

13.6 Summary

This now completes our study of multiplexing strategies. We started by giving several compelling reasons for multiplexing in modern telecommunications and then presented a nonmathematical discussion of the four strategies of SDM, FDM, TDM, and CDM. This was followed by a more detailed discussion of the last three techniques.

FDM is truly indispensable to radio communications and has a very long list of applications. It allows the existence of several audio and TV broadcast houses in one locality, and the simultaneous provision of a large variety of communication services. Capacity enhancement in cellular telephony and satellite communication relies heavily on FDM. Closed media applications of FDM include wavelength division multiplexing (WDM) in optical fibre, which allows literally millions of toll-quality digital voice signals to be transmitted in one fibre. FDM telephony allowing up to 10 800 analogue voice signals to be transmitted in one coaxial cable was popular up till the 1980s. FDM implementation is very straightforward. A frequency band is allocated to a user, and the user's signal is applied to modulate a suitable carrier thereby translating the signal into its allocated band. The type of modulation technique depends on the communication system. SSB was used in FDM telephony, on–off keying (OOK) is used in optical fibre, FM was used in first generation cellular telephony and analogue satellite communication, and M-ary APSK is used in modern satellite and terrestrial communications, etc. Each of these modulation techniques is covered in previous chapters. Our discussion of FDM included its application in telephony where a complete set of standards was specified for hierarchical implementation.

TDM fits in very well with the techniques of digital switching in modern networks and is ideally suited for transmitting digital signals or bit streams from multiple sources. It allows the advantages of digital communications to be extended to a larger number of simultaneous users in a common transmission medium than would be possible with FDM. We presented a detailed discussion of (nonstatistical) TDM optimised for digital transmission of voice, including the plesiochronous and synchronous digital hierarchies. To show how the requirements of broadband integrated services are satisfied, we presented the statistical TDM technique of ATM, which satisfactorily multiplexes all types of digital signals, including voice, data, and video. However, we noted by way of analogies that IP has beaten ATM to become the preferred transmission technology of the twenty-first century.

We also discussed various spread spectrum modulation techniques, including time-hopping, frequency-hopping, and direct sequence. In studying CDM, we demonstrated the importance of several factors, including code synchronisation and cross-correlation, power control, processing gain, and the length of the code sequence.

We concluded the chapter with a brief discussion of the application of the above multiplexing strategies for multiple access in satellite communication systems. The suitability of a multiple access technique for a given application or its superiority to other techniques is still open to debate. We briefly presented the merits and drawbacks of each technique and provided formulas for system capacity calculations. You should therefore now be better equipped to make an informed choice.

Questions

13.1 Higher line utilisation may be realised by multiplexing 16 voice signals into one 48 kHz group signal. The following procedure has been specified by the ITU for doing this. Each voice signal is limited to frequencies of 0.25–3.05 kHz. Frequency translation of each voice signal to an exclusive passband is accomplished for the odd-numbered channels using eight LSB-modulated carriers at frequencies (kHz) 63.15, 69.15, 75.15, … The even-numbered channels are translated using eight USB modulated carriers at frequencies (kHz) 62.85, 68.85, 74.85, …

(a) Draw detailed block diagrams of the multiplexer and demultiplexer for this 16-channel FDM system.
(b) Sketch a clearly labelled spectrum (similar to Figure 13.7a) of the 16-channel group signal.
(c) Determine the nominal bandwidth and GB of each voice channel.
(d) Determine the Q and $\mathbb{Z}$ factors of the most stringent filter used in this FDM system.
(e) Compare your result in (d) to that of a standard 12-channel group signal.

13.2 (a) Sketch a clearly labelled spectrum of the HG signal in the UK FDM system.
(b) Determine the Q factor of the most stringent filter in the STE of Figure 13.9.

13.3 Determine the Q and $\mathbb{Z}$ factors of the most stringent filter in a 10 800-channel UK hierarchical FDM system. How does this compare with a flat-level assembly of the same number of voice channels using subcarriers of 4 kHz spacing starting at 1 MHz?

13.4 Determine the number of CTE, GTE, and STE required to set up a 600-channel Bell FDM system. Draw a block diagram showing the connection of these devices from the second multiplexing stage.